Conference on Modelling Fluid Flow (CMFF'25)
The 19th International Conference on Fluid Flow Technologies
Budapest, Hungary, August 26-August 29, 2025

A CFD STUDY ON DEPOSITION EFFICIENCY IN CASE OF INHALED AEROSOL MEDICATION

Péter SÁFRÁNY[1], Csaba HŐS[2],

[1] Corresponding Author. Department of Hydrodynamic Systems, Faculty of Mechanical Engineering, Budapest University of Technology and Economics. Budapest University of Technology and Economics, Műegyetem rkp. 3., H-1111 Budapest, Hungary. Tel.: +36 30 994 1569, E-mail: psafrany@hds.bme.hu
[2] Department of Hydrodynamic Systems, Faculty of Mechanical Engineering, Budapest University of Technology and Economics. E-mail: hos.csaba@gpk.bme.hu

ABSTRACT

The aim of this study is to examine how the deposition efficiency of inhaled aerosol medications is affected by the varying geometrical characteristics of the extra-thoracic region. To this end, numerical simulations were performed on a realistic geometry, and on a range of simplified and modified versions. The results were compared and evaluated based on several factors, including deposition efficiency, mean velocity, turbulence intensity, overall pressure drop, and velocity profile at the exit plane. The numerical method was validated through 3D printing and measurement of the pressure drop of the realistic geometry and the geometry that performed best among the simplified geometries at the simulated flow rate. These results will facilitate the evaluation of the usability of simplified geometries for flow and particle deposition simulations, thereby enhancing patient-specific simulations where the extra-thoracic region cannot be accurately reconstructed.

Keywords: CFD, CFPD, inhaled medicine, oral airways, particle deposition

NOMENCLATURE

$UMean$	$[m/s]$	time averaged velocity magnitude
k	$[m^2/s^2]$	turbulence kinetic energy

1. INTRODUCTION

Inhaled drug particles are frequently used to treat respiratory diseases such as asthma and chronic obstructive pulmonary disease (COPD). In recent years, inhaled insulin and painkillers have also been developed. However, it is important to note that the main drawback of these devices is the precise dosing. It is evident that the quantity and distribution of the deposited drug particles are crucial for the effectiveness of the therapy. Even when a specific quantity of medication is released into the airways, as in the case of pressurized metered dose inhalers (pMDIs) or dry powder inhalers (DPIs), the deposition of particles is influenced by various factors. These include the inhalation flow rate, the patient's airway geometry, the timing of the actuation, and other variables. Over the years, numerous deposition models have been developed, including the semi-empirical model proposed by the International Commission on Radiological Protection (ICRP), known as the ICRP model [1], the 1D trumpet model, and the stochastic model, where the term 'stochastic' refers to the method of generating paths [2]. However, it is important to note that only computational fluid and particle dynamics (CFPD) simulations can consider the exact patient-specific geometry.

One potential methodology for creating patient-specific three-dimensional geometries and numerical domains involves using computed tomography (CT) or magnetic resonance imaging (MRI) alongside segmentation software capable of determining airway boundaries based on pixel values. Segmentation can be performed effectively on the trachea and the first few bifurcations. However, challenges arise during the reconstruction of the lower airways with reduced diameters and of the mouth-throat region. In the case of the lower airways, the resolution is typically insufficient for reconstruction. In the case of the mouth-throat region, the source of the difficulties lies in the complexity of the geometry [3] and the fact that patients generally keep their mouths closed during medical imaging. This leaves little to no gap for reconstruction. Consequently, reconstruction of the oral cavity and inlet boundary becomes uncertain. The inability to reconstruct the oral cavity significantly restricts research into particle deposition in patient-specific airways, since this region influences the flow properties and particle size distribution beyond the trachea. Without proper geometric modelling of the extra-thoracic region, results regarding deposition in the lower airways cannot be relied upon.

The effect of the geometry of the extra-thoracic region on the flow field and particle deposition has been extensively studied. Heenan et al. [4] demonstrated that local velocity magnitude and flow curvature greatly impact particle deposition. Significant differences occur even in the case of the same patient with different mouth openings. Grgic et al. [5] also showed that the high local velocities and rapid changes in the flow direction are key parameters for local deposition patterns. In their study, Xi et al. [6] investigated the particle deposition and flow field in a realistic oral cavity-throat geometry and its simplified versions. They simplified the overall geometry by replacing the original cross-sections with circular or elliptical ones, and their findings showed that these modifications significantly affected the local deposition patterns. The study concluded that the realistic geometry provided the most accurate deposition predictions at different flow rates. It also identified the glottis and the upper trachea as the geometric features that principally affect deposition, where the so-called laryngeal jet forms. Since the overall geometry was simplified, these features were only included in the realistic model.

Nicolau and Zaki [7] performed direct numerical simulations (DNS) on four realistic extra-thoracic geometries. They found that the flow field and deposition are affected not only by patient-specific geometric differences, but also by the position of the tongue in the case of the same subject.

Xi et al. [8] investigated the effect of total airway volume, oral cavity volume, airway curvature, and glottal area on the transport and deposition of inhaled aerosols in the mouth-throat region. They used and modified the realistic, constant-diameter and elliptical models described in [6] along with the USP IP model described in [9]. They concluded that the glottal area and total airway volume have a greater impact on deposition than curvature and oral cavity volume.

In their study, Feng et al. [10] compared seven different upper airway geometries and identified that the laryngeal jet and the recirculating zone significantly impact particle transport and deposition. Additional studies also revealed that particle deposition in the laryngeal region was enhanced by the formation of the laryngeal jet. [11, 12, 13]. Ma et al. [14] also compared modified, realistic oral cavity–throat models and found that the uvula and epiglottis have the greatest effect on particle deposition, however, the models should also incorporate the soft palate.

It can be concluded that the geometry of the throat plays a key role in the flow characteristics entering the trachea, as well as in particle deposition patterns. Since the throat can be reconstructed from medical images, the aim of this study is to investigate the potential application of a simplified oral cavity in patient-specific particle deposition studies. The main expectation of the simplified geometry is that it should be easily adapted to the reconstructed airways, provide realistic flow characteristics at the tracheal inlet and correctly model the particle filtration properties of the extra-thoracic region. To this end, the flow field and deposition patterns in a realistic extra-thoracic geometry were compared with the results of three simplified oral cavity cases.

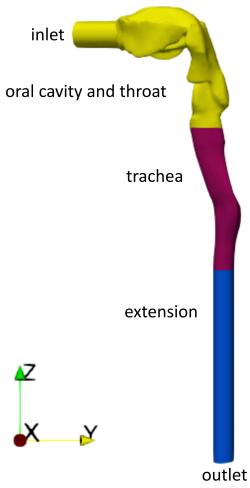

Figure 1. The complete original geometry.

2. NUMERICAL METHODS

2.1. Geometry and the numerical mesh

The geometry of the oral cavity, throat, and trachea is the same as in the SimInhale benchmark case [15]. The trachea was lengthened by 140 mm to minimise the impact of the outlet boundary condition on the flow upstream. The full original geometry (*og*) can be seen in Figure 1. Simplified geometries have been created for our investigation to study the impact of on the simplification of the oral cavity. The inlet of the *og* starts with a 20 mm diameter pipe section, which forms the basis for all the modified geometries. The center line of the *og* was calculated using the VMTK Python package, then the original oral cavity was removed with a plane cut just above the epiglottis. The center line and exact location of the cut are indicated in Figure 2.

The first simplified geometry (*sg1*) was created by extending the inlet, followed by a 90° loft along the center line to the cutoff. In contrast, for the second simplified geometry (*sg2*), involved sweeping the inlet cross-section along the center line and lofting it to the cutoff. The third simplified geometry (*sg3*) featured a swept inlet section and a swept cutoff lofted together. For *sg3*, the sweeps were performed along the lower outline in the YZ section of the original oral cavity rather than along the center line. Side and top views of the simplified geometries can be seen in Figure 3 and 4. As can be seen in Fig 3 and 4, the spaces surrounding the teeth have been completely eliminated, significantly reducing the com-

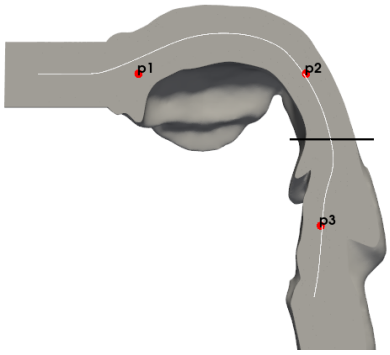

Figure 2. Cross-sectional view of the oral cavity and throat, showing the centerline (white), the location of the plane section cut (black) and the pressure sampling points (red marks).

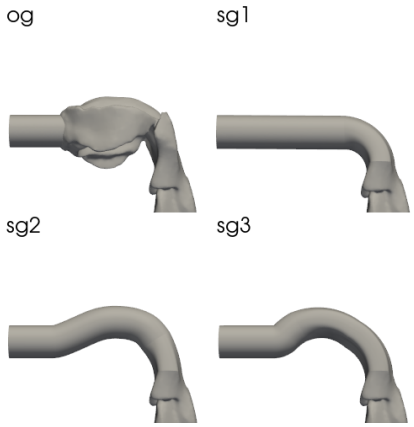

Figure 3. Simplified geometric shapes viewed from the side.

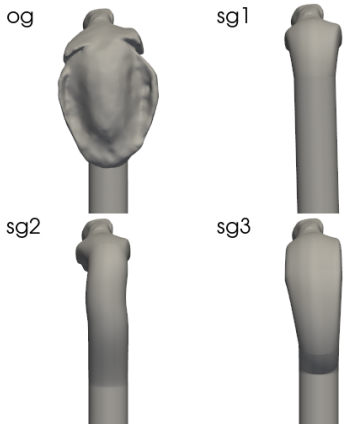

Figure 4. Simplified geometric shapes viewed from the top.

plexity of the domain.

The numerical mesh for the created models was generated using the built-in snappyHexMesh utility in OpenFOAM. Five boundary layer cells were added to the walls, with the height of the first cell set to 60 μm and an expansion ratio of 1.2. Spasov et al. [16] demonstrated that this configuration is adequate for accurately resolving the boundary layer in this geometry.

2.2. Flow field

Numerical simulations were conducted using the OpenFOAM software package. A 60 L/min flow rate and a zero-pressure gradient were set at the inlet for each case, while the outlet boundary conditions were set to zero static pressure and zero velocity gradient. Given that the flow is turbulent at this flow rate, the k-ω SST model was selected for the turbulence modelling. This model performs well in the near wall region but might underestimate the turbulent kinetic energy levels [17]. A commonly applied [16, 18, 17] turbulence intensity of 5% was introduced at the inlet and the omegaWallFunction was applied to the walls to properly model the boundary layer. This wall function calculates the local y+ value and adjusts its parameters accordingly. This is highly beneficial, as both low- and high-velocity zones occur in the geometry.

The used numerical schemes have been adopted from the work of Spasov et al. [16]. The authors demonstrated that the complexity of the geometry prevents achieving a proper steady-state solution, therefore, averaging the flow field from the unsteady solution is the best approach. To achieve this, unsteady simulations lasting 0.5 seconds were conducted using the PIMPLE algorithm, and the flow fields were averaged over all the time steps to obtain mean values.

A grid independence study was conducted on the *og* using three different mesh resolutions. The pressure was monitored in three locations shown in Fig 2. Table 1 presents the results of the grid independence study. The results demonstrate good agreement, with the highest relative deviation between the medium and fine meshes being 3.46% at the third sampling point. Therefore, the medium mesh was accepted for the numerical studies.

Table 1. Mesh independence study results

	Million cells	p1, Pa	p2, Pa	p3, Pa
coarse	3.533	52.51	48.01	27.58
medium	4.686	52.82	48.41	28.03
fine	6.293	53.77	49	29.03

2.3. Particle dynamics

After solving the flow field, the passive transport and deposition of kinematic particles were investigated. The equation of motion for the particles

was solved using the icoUncoupledKinematicParcelFoam solver on the averaged velocity and pressure field. The particles were introduced at the inlet patch with a uniform size distribution. The particle density was set to 1.23 kg/m³, with the smallest diameter set to 1 μm and the largest to 15 μm. The particles had an initial velocity of 40 m/s in the x-direction, with a release duration of 0.1 seconds. These values correspond to the particle size range and velocity released from a pMDI device [19]. A total of 180,000 particles were injected into the domain. Stick interaction was set for the walls, meaning a particle was considered deposited as soon as it hit the wall. The stochasticDispersionRAS model was used to account for turbulence. Each particle was tracked individually and the maximum particle Courant number was set to 5e-3.

3. MESUREMENTS

In order to validate the simulations and determine the effect of simplification on the resistance of the mouth-throat region, the average pressure was measured at the tracheal inlet. Square time-flow curves were generated using a Piston Medical PWG-33 pulmonary waveform generator, and the pressure difference was measured with a Sensirion SDP31 differential pressure sensor. The *og* and *sg2* oral cavity and throat regions were 3D-printed using DLP technology. A short channel with eight pressure sampling ports was added at the exit of the throat to measure the average pressure in the cross-section. The measurement setup is shown below in Fig 5.

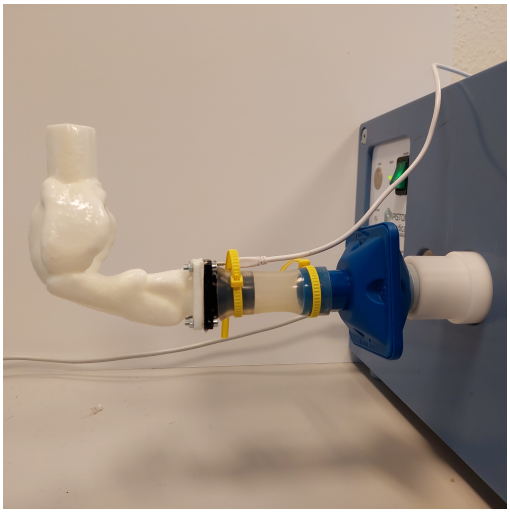

Figure 5. Measurement setup

4. RESULTS

4.1. Velocity field and pressure drop

Simplifying the oral cavity is advantageous from both a reconstruction perspective and because it requires fewer numerical cells, thereby reducing simulation times. The difference in run time was noticeable in particle simulations, where the simplified

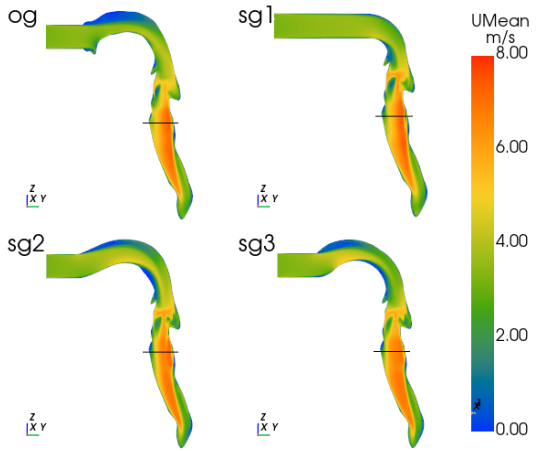

Figure 6. Velocity distribution on the YZ plane

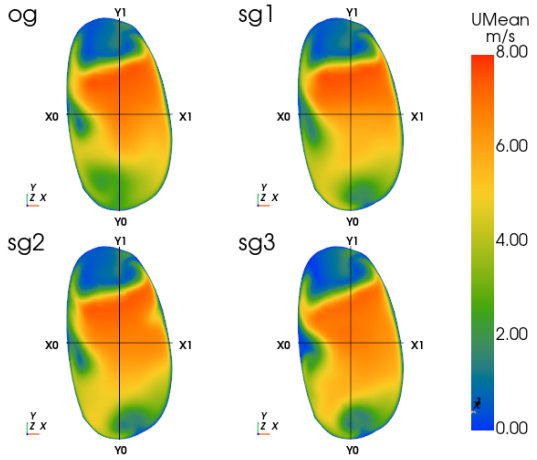

Figure 7. Velocity distribution at the inlet of the trachea.

geometry simulations were, on average, 25% faster.

As emphasized in the introduction, jet formation in the larynx significantly impacts the flow pattern in the trachea and consequently affects flow in the downstream airways. Therefore, a key feature of the simplified geometry should be its ability to produce the same flow pattern at the tracheal inlet.

Figure 6 shows the mean velocity on the YZ plane. The centreline of the original geometry does not fully lie in the YZ plane, which is why the full cross-section has not been included. As can be seen, there is no significant difference in velocity magnitude between the original and simplified cases. The main differences can be observed in the cases of *sg2* and *sg3*, a higher velocity can be seen above the tongue's arc, and the flow separates immediately thereafter. In the case of *sg1*, the separation occurs just before the epiglottis, which reduces its impact on the flow.

Figure 7 and Figure 8 show the mean velocity and turbulence kinetic energy (TKE) distributions at the inlet of the trachea in the latest timestep. The precise location of the sections shown in Fig. 6 is indicated by a black line. The main difference between

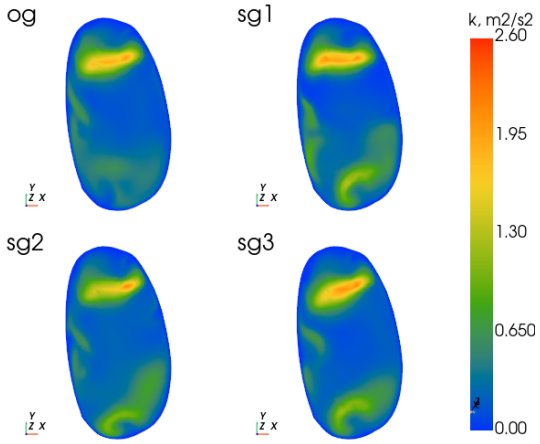

Figure 8. Turbulent kinetic energy distribution at the inlet of the trachea.

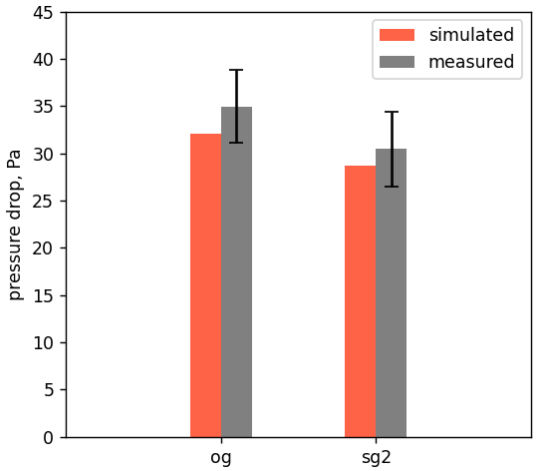

Figure 9. Simulated and measured pressure difference in the *og* and *sg2* oral cavity - throat models

the *og* and the simplified versions can be seen in the shape of the recirculating zones. Other than that, there is no significant difference in the observed velocity distributions. For correct particle deposition results, a proper turbulence kinetic energy distribution is essential [16]. As can be observed in Fig. 8, it is striking that close to the walls on the bottom side, all three simplified geometries generate a much higher local TKE. This is certainly a considerable factor when using simplified geometries.

To gain a more comprehensive understanding of the velocity distribution, the velocity components have been plotted along the X0-X1 and Y0-Y1 lines, as shown in Fig 7. Plots of the velocity components can be seen in Figure 10 and 11. As demonstrated by the velocity magnitude plots, it is not surprising that the z component of the velocity agrees with the original and simplified geometries. Along the X0-X1 line, none of the simplified cases are close to the original geometry with regard to the x component of the velocity. The *sg2*, however, aligns well with the y component. Along the Y0-Y1 line, it is also noteworthy that the x component of all the simplified cases is erroneous in the vicinity of the wall at Y0. Based on the velocity profiles, *sg2* was selected as the most appropriate simplification of the three models investigated.

In the case of the *og*, the simulated and measured pressure differences at 60 L/min between the inlet and the tracheal inlet were 32.06 Pa and 34.97 ±3.86 Pa, respectively. For the *sg2* these values were 28.72 Pa and 30.44 ±3.92 Pa. Considering the unsteadiness of the flow and the uneven pressure distribution in the exit plane, the measured and simulated results are in good agreement. Figure 9 demonstrates the simulated and measured pressure differences for the two models.

4.2. Deposition of particles

The fundamental expectation when employing a simplified oral cavity is that the filtration of particles should be equivalent to that of the original geometry. To investigate this property of simplified geometries, the number of particles deposited in the oral cavity and throat was summed. Histograms of the size distribution of the deposited particles were plotted based on the absolute and normalized particle counts. Normalization was based on particle counts for the *og*. These are shown in Figure 12 and 13.

Using simplified geometries has been shown to significantly reduce particle deposition across all diameters. This finding is somewhat counter-intuitive given the lack of observed differences in the flow field. Relative filtration varies greatly from diameter to diameter, peaking around 5 to 7 μm. Below this, there are large fluctuations, but this is due to the relatively low number of deposited particles. Above 8 μm it remains nearly constant.

Whether simplified geometries can be used will ultimately be determined by whether the same tend-

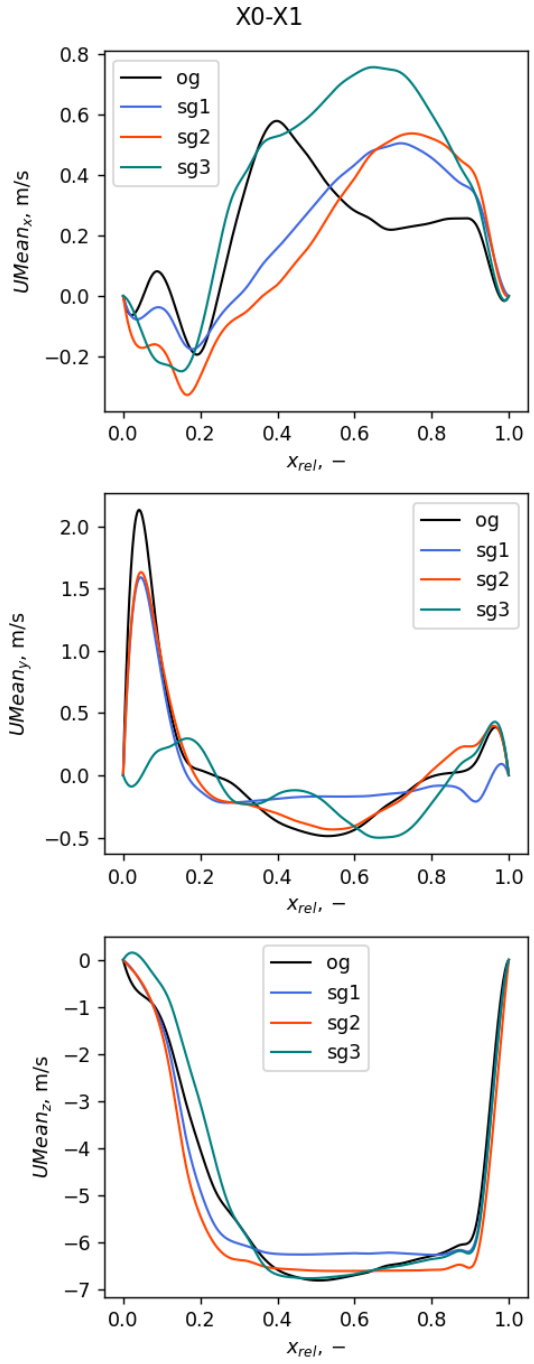

Figure 10. Velocity components along X0-X1

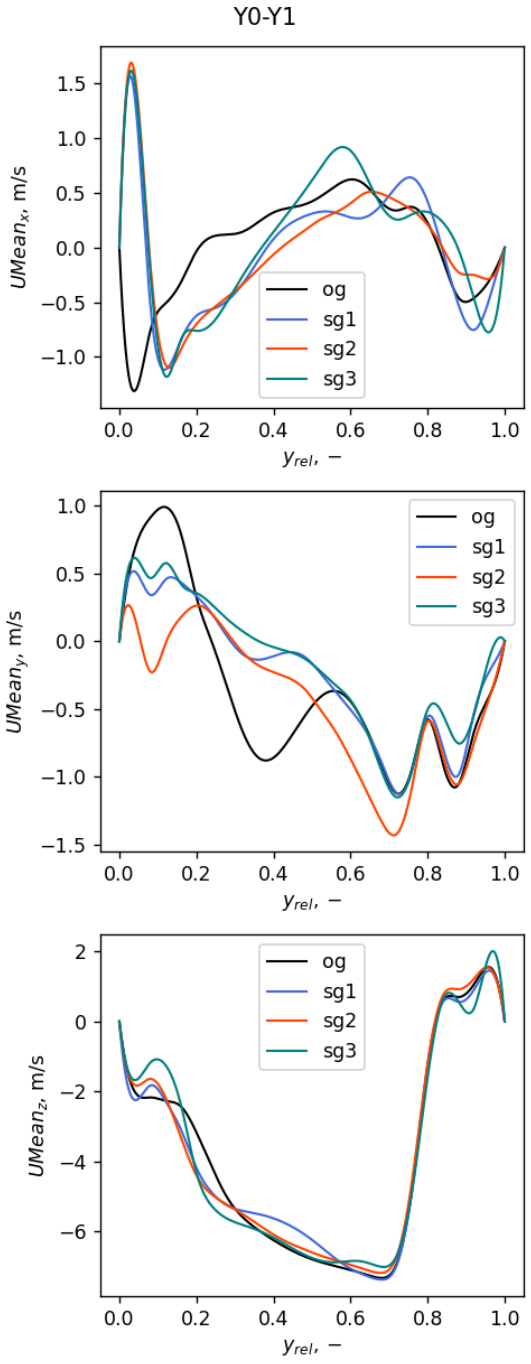

Figure 11. Velocity components along Y0-Y1

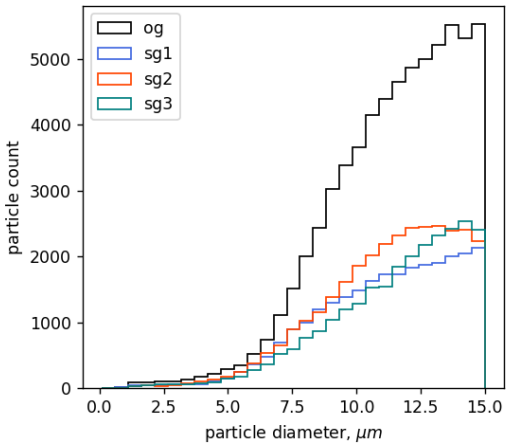

Figure 12. Histogram of the deposited particles in the oral cavity and the throat

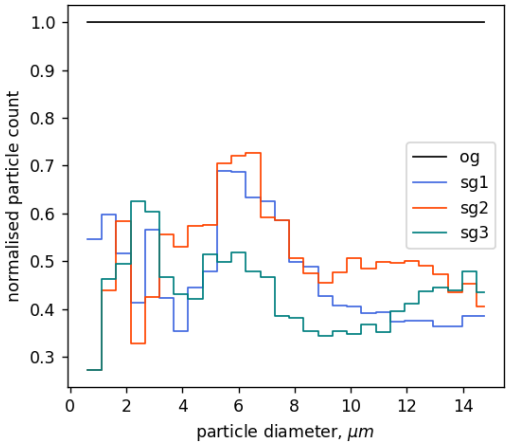

Figure 13. Normalized histogram of the deposited particles in the oral cavity and the throat

ency can be observed for other realistic oral cavity geometries. To enhance the overall performance of the simplification, a more robust and detailed analysis is required. However, it should be noted that such an analysis falls outside the scope of this study.

5. CONCLUSION

In this study, the authors investigated the usability of simplified oral cavity geometries. To this end, numerical unsteady simulations were carried out at a constant flow rate. The study concluded that the geometry of the oral cavity has little to no influence on the velocity field downstream of the throat at the inlet of the trachea. Furthermore, simplification reduced the resistance of the investigated region, which was validated by measurements. These findings are particularly beneficial for flow simulations in the airways, given the significance of the tracheal flow profile for flow distribution and particle deposition in the lower airways.

However, particle deposition simulations revealed limitations of the simplification, as the number of deposited particles was underestimated in the simplified geometries compared to the original geometry.

Further research is necessary to improve the performance of simplified oral cavities. This will involve conducting parameter studies at multiple flow rates and investigating the flow field in greater detail. These investigations will form the basis of future work.

ACKNOWLEDGEMENTS

Project no. kdp-ikt-2023-900-i1-00000957/0000003 has been implemented with the support provided by the Ministry of Culture and Innovation of Hungary from the national research, development and innovation fund, financed under the kdp-2023 funding scheme.

The scientific work/research and/or results publicised in this article were reached with the sponsorship of the Gedeon Richter Talentum Foundation in the framework of the Gedeon Richter Excellence PhD Scholarship of Gedeon Richter.

We acknowledge the Digital Government Development and Project Management Ltd. for awarding us access to the Komondor HPC facility based in Hungary.

REFERENCES

[1] ICRP, 1994, “Human Respiratory Tract Model for Radiological Protection”, *ICRP Publication 66 Ann ICRP 24 (1-3)*.

[2] Hofmann, W., 2011, “Modelling inhaled particle deposition in the human lung—A review”, *Journal of Aerosol Science*, Vol. 42 (10), pp. 693–724.

[3] Koullapis, P., Nicolaou, L., and Kassinos, S., 2018, “In silico assessment of mouth-throat effects on regional deposition in the upper tracheobronchial airways”, *Journal of Aerosol Science*, Vol. 117, pp. 164–188.

[4] Heenan, A. F., Finlay, W. H., Grgic, B., Pollard, A., and Burnell, P. K., 2004, “An investigation of the relationship between the flow field and regional deposition in realistic extra-thoracic airways”, *Journal of Aerosol Science*, Vol. 35, pp. 1013–1023.

[5] Grgic, B., Finlay, W. H., Burnell, P. K., and Heenan, A. F., 2004, “In vitro intersubject and intrasubject deposition measurements in realistic mouth–throat geometries”, *Journal of Aerosol Science*, Vol. 35, pp. 1025–1040.

[6] Xi, J., and Longest, P. W., 2007, “Transport and deposition of micro-aerosols in realistic and simplified models of the oral airway”, *Annals of Biomedical Engineering*, Vol. 35, pp. 560–581.

[7] Nicolaou, L., and Zaki, T. A., 2013, "Direct numerical simulations of flow in realistic mouth–throat geometries", *Journal of Aerosol Science*, Vol. 57, pp. 71–87.

[8] Xi, J., Yuan, J. E., Yang, M., Si, X., Zhou, Y., and Cheng, Y. S., 2016, "Parametric study on mouth–throat geometrical factors on deposition of orally inhaled aerosols", *Journal of Aerosol Science*, Vol. 99, pp. 94–106.

[9] Pharmacopeia, U., 2005, "Physical tests and determinations: Aerosols, nasal sprays, metered-dose inhalers, and dry powder inhalers", *United States Pharmacopeia First Supplement, 28-NF, General Chapter (601)*, p. 3298 – 3316, cited by: 6.

[10] Feng, Y., Zhao, J., Kleinstreuer, C., Wang, Q., Wang, J., Wu, D. H., and Lin, J., 2018, "An in silico inter-subject variability study of extrathoracic morphology effects on inhaled particle transport and deposition", *Journal of Aerosol Science*, Vol. 123, pp. 185–207.

[11] Koullapis, P., Kassinos, S., Bivolarova, M., and Melikov, A., 2016, "Particle deposition in a realistic geometry of the human conducting airways: Effects of inlet velocity profile, inhalation flowrate and electrostatic charge", *Journal of Biomechanics*, Vol. 49 (11), pp. 2201–2212, selected Articles from the International Conference on CFD in Medicine and Biology (Albufeira, Portugal – August 30th - September 4th, 2015).

[12] Atzeni, C., Lesma, G., Dubini, G., Masi, M., Rossi, F., and Bianchi, E., 2021, "Computational fluid dynamic models as tools to predict aerosol distribution in tracheobronchial airways", *Scientific Reports 2021 11:1*, Vol. 11, pp. 1–13.

[13] Worth Longest, P., and Vinchurkar, S., 2007, "Validating CFD predictions of respiratory aerosol deposition: Effects of upstream transition and turbulence", *Journal of Biomechanics*, Vol. 40 (2), pp. 305–316.

[14] Ma, Z., Kourmatzis, A., Milton-McGurk, L., Chan, H.-K., Farina, D., and Cheng, S., 2022, "Simulating the effect of individual upper airway anatomical features on drug deposition", *International Journal of Pharmaceutics*, Vol. 628, p. 122219.

[15] Koullapis, P., Kassinos, S., Muela, J., Perez-Segarra, C., Rigola, J., Lehmkuhl, O., Cui, Y., Sommerfeld, M., Elcner, J., Jicha, M., Saveljic, I., Filipovic, N., Lizal, F., and Nicolaou, L., 2018, "Regional aerosol deposition in the human airways: The SimInhale benchmark case and a critical assessment of in silico methods", *European Journal of Pharmaceutical Sciences*, Vol. 113, pp. 77–94, a special issue dedicated to COST Action SimInhale: cross-disciplinary perspective on the current state of the art and challenges in pulmonary drug delivery.

[16] Spasov, G. H., Rossi, R., Vanossi, A., Cottini, C., and Benassi, A., 2022, "A critical analysis of the CFD-DEM simulation of pharmaceutical aerosols deposition in extra-thoracic airways", *International Journal of Pharmaceutics*, Vol. 629, p. 122331.

[17] Sommerfeld, M., Sgrott, O., Taborda, M., Koullapis, P., Bauer, K., and Kassinos, S., 2021, "Analysis of flow field and turbulence predictions in a lung model applying RANS and implications for particle deposition", *European Journal of Pharmaceutical Sciences*, Vol. 166, p. 105959.

[18] Bass, K., and Worth Longest, P., 2018, "Recommendations for simulating microparticle deposition at conditions similar to the upper airways with two-equation turbulence models", *Journal of Aerosol Science*, Vol. 119, pp. 31–50.

[19] Talaat, M., Si, X., and Xi, J., 2022, "Effect of MDI Actuation Timing on Inhalation Dosimetry in a Human Respiratory Tract Model", *Pharmaceuticals*, Vol. 15 (1).